ISSN No:-2456-2165 https://doi.org/10.38124/ijisrt/26feb1444

Investigation of the Corrosion Behavior of Wire Arc Additively Manufactured AA7075 Nano-TiC Metal Matrix Composite

Arulkumar S.[1*]; Anandakrishnan V.[2]; Jayasankari S.[3]

[1]Aeronuatical Development Agency, Bangalore, Karnataka 560017, India.
[2]National Institute of Technology Tiruchirappalli, Tiruchirappalli, Tamil Nadu, India.
[3]School of Computing, SASTRA Deemed to be University, Thanjavur, Tamil Nadu, India.

Corresponding Author: Arulkumar S.[1*]

Publication Date: 2026/03/06

Abstract: Additive manufacturing enables near net-shape fabrication with reduced material waste, supporting sustainable and lean manufacturing practices for rapid component production and repair. In the present study, wire arc additive manufacturing (WAAM) using a gas metal arc welding process was employed to fabricate an AA7075 aluminum alloy reinforced with nano-sized titanium carbide (TiC) particles. The corrosion behavior of the WAAM-fabricated AA7075–Nano-TiC metal matrix composite was systematically investigated in 3.5 wt.% NaCl solution and correlated with microstructural characteristics. Electron backscatter diffraction analysis was performed to examine grain morphology, while hardness measurements were used to assess mechanical response. Electrochemical corrosion behavior was evaluated using potentiodynamic polarization and electrochemical impedance spectroscopy techniques. The corrosion potential and corrosion current density were determined using Tafel extrapolation, while impedance behavior was analyzed through Bode impedance and phase angle plots. The WAAM-fabricated composite exhibited moderate corrosion resistance, governed by charge transfer through a non-ideal passive oxide layer. Scanning electron microscopy coupled with energy-dispersive spectroscopy was used to examine the corroded surface morphology and elemental distribution. The results highlight the influence of WAAM-induced microstructural heterogeneity and nano-TiC reinforcement on the corrosion behavior of AA7075-based composites.

Keywords: *AA7075 Nano-TiC Metal Matrix Composite, Wire Arc Additive Manufacturing, Corrosion Behavior, Potentiodynamic Polarization, Electrochemical Impedance Spectroscopy.*

How to Cite: Arulkumar S.; Anandakrishnan V.; Jayasankari S. (2026) Investigation of the Corrosion Behavior of Wire Arc Additively Manufactured AA7075 Nano-TiC Metal Matrix Composite. *International Journal of Innovative Science and Research Technology,* 11(2), 2701-2710. https://doi.org/10.38124/ijisrt/26feb1444

I. INTRODUCTION

Rapid prototyping and near net-shape manufacturing of complex metallic components have traditionally relied on powder bed fusion–based additive manufacturing techniques. Despite their ability to fabricate intricate geometries, these processes suffer from inherent limitations such as high powder costs, elevated energy consumption, and size constraints, which restrict their application in large-scale structural components [1,2]. To overcome these challenges, alternative additive manufacturing routes including selective laser melting, electron beam melting, and direct energy deposition have been developed [3,4]. Among these, wire arc additive manufacturing (WAAM) has gained significant attention owing to its high deposition rate, reduced material wastage, and economic feasibility for fabricating large components [5,6].

WAAM employs an arc welding heat source to enable layer-by-layer deposition, making it particularly suitable for structural metals. Gas metal arc welding (GMAW)–based WAAM is widely adopted due to its stable arc characteristics, high arc energy efficiency, and process simplicity [7]. A broad range of materials, including steels, aluminum alloys, titanium alloys, and nickel-based superalloys, can be processed using WAAM [8–10]. In recent years, aluminum alloys have attracted considerable interest for WAAM applications due to their low density and high specific strength, which are critical for aerospace and transportation sectors [11].

Among aluminum alloys, AA7075 is extensively used in aerospace structures owing to its superior strength-to-weight ratio. However, the presence of alloying elements such as zinc, magnesium, and copper makes AA7075

ISSN No:-2456-2165 https://doi.org/10.38124/ijisrt/26feb1444

susceptible to localized corrosion, particularly in chloride-containing environments [12,13]. The corrosion behavior of AA7075 is strongly influenced by microstructural features such as grain size, intermetallic phase distribution, and passive film stability [14]. Additive manufacturing processes, including WAAM, introduce non-equilibrium solidification, elemental segregation, and porosity, which further affect corrosion performance [15,16].

To enhance mechanical and functional properties, ceramic reinforcements have been incorporated into aluminum matrices to form metal matrix composites. Titanium carbide (TiC) has emerged as a promising reinforcement due to its high hardness, chemical stability, and compatibility with aluminum alloys [17,18]. Nano-sized TiC particles are particularly effective in promoting grain refinement and improving hardness through particle pinning and load transfer mechanisms [19]. However, the introduction of ceramic reinforcements may also influence corrosion behavior by modifying passive film characteristics and creating heterogeneous reinforcement–matrix interfaces [20].

Previous studies on additively manufactured aluminum and titanium alloys have reported reduced corrosion resistance compared to their wrought counterparts, primarily due to the formation of defective passive films and increased density of microstructural discontinuities [21,22]. Corrosion-resistant materials rely on the formation of stable and continuous oxide layers to protect against aggressive environments, and disruption of these layers accelerates localized corrosion [23]. Investigations on additively manufactured alloys processed via laser- and arc-based techniques have shown that porosity, molten pool boundaries, and secondary phase formation act as preferential sites for corrosion initiation [24,25].

Although WAAM processing has been reported to enhance mechanical properties such as hardness through repeated thermal cycling and grain refinement [26,27], the associated non-equilibrium microstructures and residual stresses may adversely affect corrosion behavior. Studies have indicated that while reinforcement-induced grain refinement improves mechanical response, micro-galvanic coupling between ceramic reinforcements and the aluminum matrix can deteriorate corrosion resistance in chloride environments [28]. Despite the growing interest in WAAM-fabricated aluminum matrix composites, systematic investigations on the corrosion behavior of WAAM-processed AA7075 reinforced with nano-sized TiC particles remain limited.

Therefore, the present study focuses on the fabrication of AA7075–Nano-TiC metal matrix composites using the WAAM process and a comprehensive evaluation of their corrosion behavior in 3.5 wt.% NaCl solution. Potentiodynamic polarization and electrochemical impedance spectroscopy techniques are employed to assess corrosion performance, and the results are correlated with microstructural characteristics. Scanning electron microscopy coupled with energy-dispersive spectroscopy is used to examine the morphology and elemental distribution of the corroded surfaces.

II. EXPERIMENTAL WORK

➢ *Materials and Methods*

A six-axis robotic welding system (ABB IRG 1520ID) integrated with a Fronius TPSi 400A welding power source was employed to carry out the wire arc additive manufacturing (WAAM) process for single-pass multilayer deposition, as schematically illustrated in Fig. 1. The WAAM process was selected to enable continuous and controlled deposition using a nano-treated AA7075–TiC filler wire. The filler wire, with a diameter of 1.2 mm and containing 1 wt.% titanium carbide (TiC), was procured from M/s Metal Li, USA. An annealed AA7075 aluminum alloy plate with a thickness of 25 mm was used as the substrate material. Prior to deposition, the filler wire was characterized using scanning electron microscopy (SEM) and energy-dispersive spectroscopy (EDS) to confirm the presence and distribution of nano-sized TiC particles, and the corresponding compositional details are summarized in Table 1.

Table 1 Elemental Composition (1wt.%) of Nano-Treated AA7075 Filler Material

Materials	Zn	Mg	Cr	Cu		Si	Fe	Mn	Ti	Al
NT 7075-TiC	5.3	2-6	0.22	1.7		0.4	0.5	0.03	0.2	Bal.

A series of preliminary screening experiments were conducted to establish a stable operating window for the WAAM deposition process. The selection of process parameters was based on arc stability, uniform metal transfer, continuous bead formation, minimal spatter, and the absence of visible defects such as lack of fusion or excessive penetration. A satisfactory parameter range was identified when the deposited beads exhibited uniform morphology with consistent reinforcement width, controlled penetration, and uninterrupted arc behavior. These criteria were used to define the acceptable parameter limits for subsequent full factorial experimental design.

Based on the WAAM process parameters optimized using Grey Relational Analysis and the Technique for Order Preference by Similarity to Ideal Solution (TOPSIS), confirmatory experiments were performed under the predicted optimal conditions. The optimized parameters wire feed rate of 8 m/min, welding speed of 150 mm/min, and arc length correction (ALC) of −5% were employed to fabricate single-bead deposits. The experimentally measured bead width, reinforcement height, and cross-sectional area were compared with the corresponding predicted values obtained from the optimization model. The selected optimized parameters, corresponding to an operating voltage of 15.3 V, were validated based on improved deposition characteristics, including continuous bead formation, absence of lack-of-

ISSN No:-2456-2165 https://doi.org/10.38124/ijisrt/26feb1444

fusion defects, minimal surface waviness, and negligible spatter.

For the fabrication of multilayer deposits, the WAAM process was carried out at a voltage of 15.3 V, wire feed rate of 8 m/min, and welding speed of 150 mm/min. Argon was used as the shielding gas, as established during preliminary trials. An AA7075 aluminum alloy substrate with dimensions of 300 mm × 120 mm × 25 mm was used for the deposition process. The substrate thickness of 25 mm was selected to prevent distortion during deposition. The final deposited wall exhibited a thickness of 12 mm, a length of 160 mm, and a height of 35 mm. A total of eighteen layers were deposited, with an average bead height of approximately 1.94 mm per layer.

Specimens were prepared using standard metallographic procedures, followed by fine polishing to achieve a mirror finish. Microstructural analysis was performed using optical microscopy and scanning electron microscopy (SEM). The distribution of nano-TiC particles and secondary phases was examined using energy-dispersive X-ray spectroscopy (EDS). Grain orientation and grain boundary characteristics were analyzed using electron backscatter diffraction (EBSD).

➢ *Corrosion Study*

Electrochemical corrosion tests were conducted in 3.5 wt.% NaCl solution at room temperature using a three-electrode electrochemical workstation. The WAAM AA7075–Nano-TiC specimen served as the working electrode, a saturated calomel electrode (SCE) as the reference electrode, and a platinum counter electrode.

Prior to testing, samples were immersed in the electrolyte for 30 min to stabilize the open circuit potential (OCP). Potentiodynamic polarization tests were carried out at a scan rate of 1 mV/s within a suitable potential range relative to OCP. Corrosion potential (E_{corr}) and corrosion current density (i_{corr}) were determined using Tafel extrapolation. Electrochemical impedance spectroscopy (EIS) measurements were performed over a frequency range of 10^{-1} to 10^{5} Hz, and the obtained data were analyzed using Bode and phase angle plots.

III. RESULTS AND DISCUSSION

A. Electron Back Scattered Diffraction- Grain Size Measurement and Distribution Analysis

The AA7075 – Nano-TiC composite fabricated with WAAM had a finer grain size than that produced by conventional processing of AA7075, due to the effects of rapid solidification and the pinning of grains at the nano-scale due to TiC particles as indicated Figure 1 (a) (b). A higher proportion of high angle grain boundaries (HAGBs) were detected using EBSD analysis, which can have significant influences on both the mechanical properties and corrosion behavior of materials. A uniform distribution of the TiC nanoparticles throughout the Al matrix was identified using SEM-EDS, however, localized agglomeration of the TiC nanoparticles was noted in some areas.

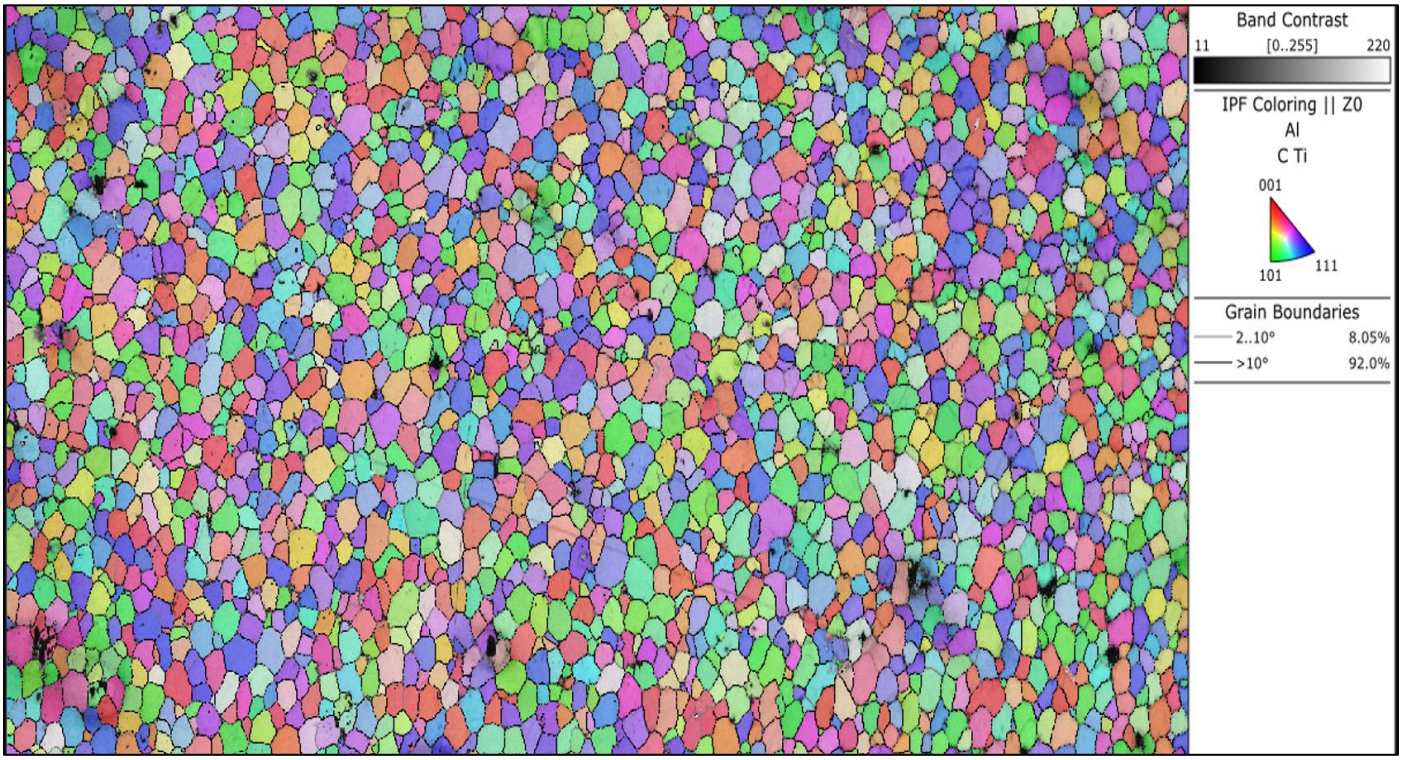

ISSN No:-2456-2165 https://doi.org/10.38124/ijisrt/26feb1444

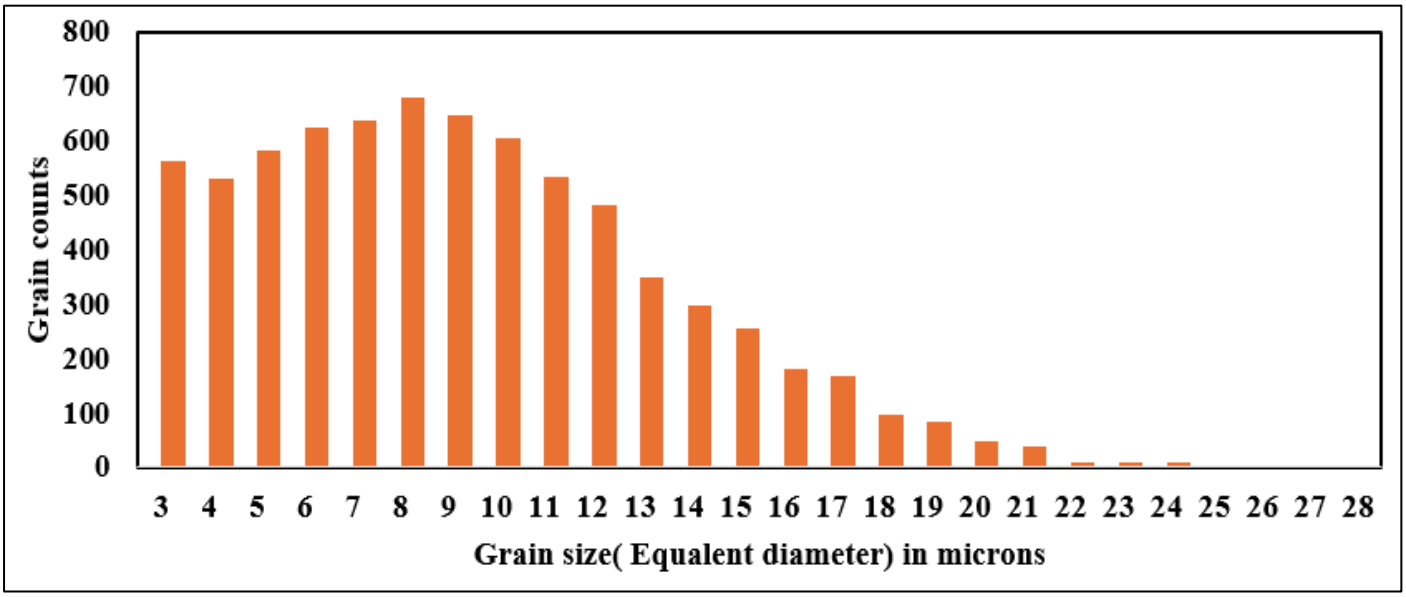

Fig 1 EBSD Analysis (a) Grain Boundary (b) Grain Size Distribution

B. Hardness Study

The WAAM-fabricated AA7075–Nano-TiC metal matrix composite exhibited an average microhardness of 104 ± 5 HV, whereas the corresponding unreinforced AA7075 alloy showed a hardness of 80 ± 5 HV. The hardness of the WAAM-deposited composite was approximately 31% higher than that of the unreinforced AA7075 Alloy. The average Vickers microhardness recorded in the deposited pass regions was 93.5 ± 9.0 HV. Therefore, it can be stated that there is an overall uniformity of hardness through the WAAM build, with little evidence of interlayer softening. The slight increase in hardness at the interlayer region is thought to arise from both localized grain size reduction and thermal cycling as each subsequent layer is deposited. This also confirmed the incredibly low standard deviation which supports the high degree of repeatability and the overall consistent mechanical response throughout the WAAM build.

C. Corrosion Study

➢ *Potentiodynamic Polarization Behavior*

Potentiodynamic polarization curves indicated the presence of an active–passive transition for the WAAM AA7075–Nano-TiC composite. The corrosion potential was shifted slightly toward the noble direction compared to unreinforced WAAM AA7075, suggesting improved thermodynamic stability. However, an increase in corrosion current density was observed in some regions, indicating susceptibility to localized corrosion, due to micro-galvanic coupling between the aluminum matrix and TiC particles or intermetallic phases. The Potentio dynamic Polarization Curve shows evidence of an Active-Passive Transition that is typical for Aluminum Alloys Exposed to Chloride Media in Figure 2.

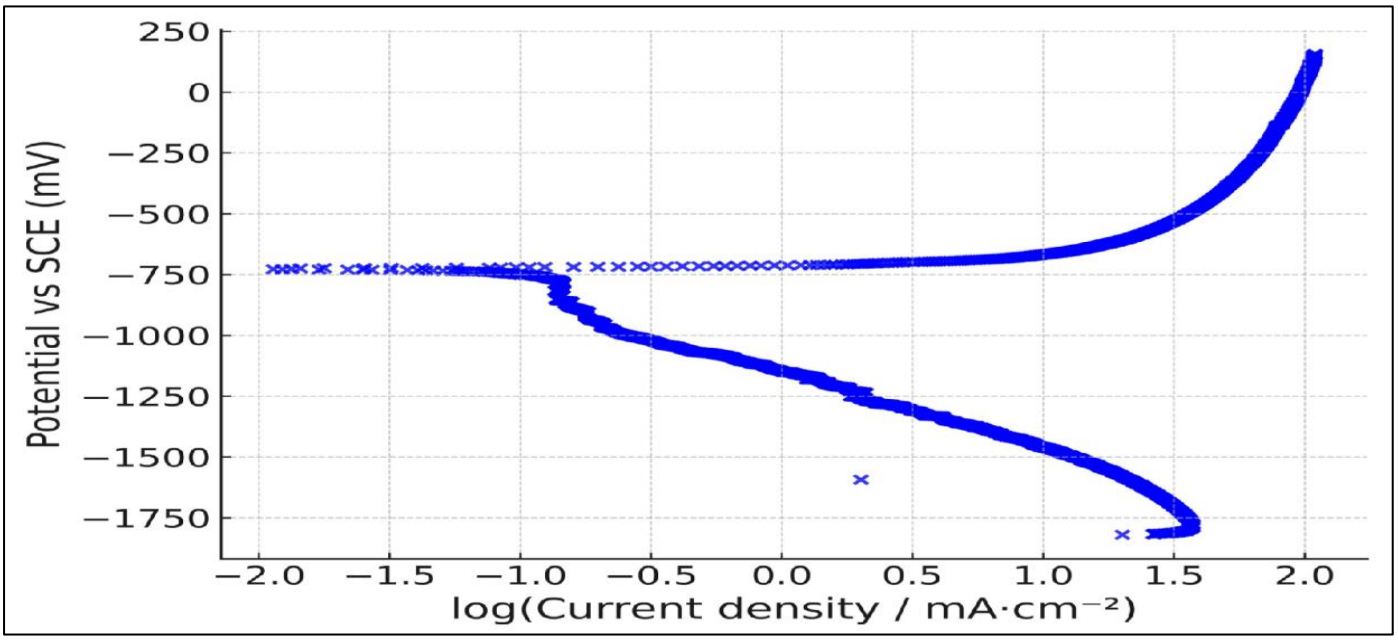

Fig 2 Potentio Dynamic Polarization Curve of the AA7075 Nano-TiC Metal Matrix Composite

ISSN No:-2456-2165 https://doi.org/10.38124/ijisrt/26feb1444

Corrosion Potential (Ecorr) is shown at approximately -750 mV vs. SCE, indicating a thermodynamic Tendency of the WAAM AA7075-Nano-TiC Composite towards the Initiation of Corrosion.

Following the Active Dissolution Region there is a clear indication of a Passive Region, showing the Formation of a Surface Oxide Film; however, the Current Density within this Passive Region Remains Relatively High, Suggesting Limited Stability of the Passive Film.

Breakdown of the Passive Film at Higher Anodic Potentials Indicate the Onset of Localized Corrosion, Primarily Pitting, as Observed through EIS. The Elevated Anodic Current Density at Higher Potentials are Likely Due to (i) Chloride-Induced Rupture of the Passive Film (ii)Particle Agglomeration of Nano-TiC Particles Acting as Preferable Pit Initiation Sites and (iii)WAAM Induced Residual Stresses Accelerating Failure of the Oxide Film.

➢ *Electrochemical Impedance Spectroscopy Analysis*

- *Bode Impedance Response*

The Bode impedance magnitude plot (Fig. X(a)), represents the electrochemical response of the WAAM-fabricated AA7075-Nano-TiC composite as it interacts with 3.5 wt.% NaCl solution as a function of frequency. The impedance modulus (|Z|) at low frequencies (10^{-2}–10^{-1} Hz) reaches an approximate maximum value of 370-380 Ω that is reflective of the overall corrosion resistance due primarily to the charge transfer process occurring at the metal – electrolyte interface. As frequency increases, the impedance modulus decreases, which represents a change from charge transfer controlled corrosion at low frequencies to a solution resistance-controlled corrosion at high frequencies. The impedance modulus at low frequencies is moderately low; this may represent some degree of breakdown of the passive oxide layer on the surface of the metal, which can be attributed to the micro structural heterogeneity and the reinforcement-matrix interfaces resulting from the WAAM processing technique as indicated in Figure 3.At high frequencies (>10^3 Hz) the impedance modulus becomes stable at a lower value (approximately 10–15 Ω), which represents the electrolyte resistance (Rs). This demonstrates that the data is reliable and there are no inductive effects present.

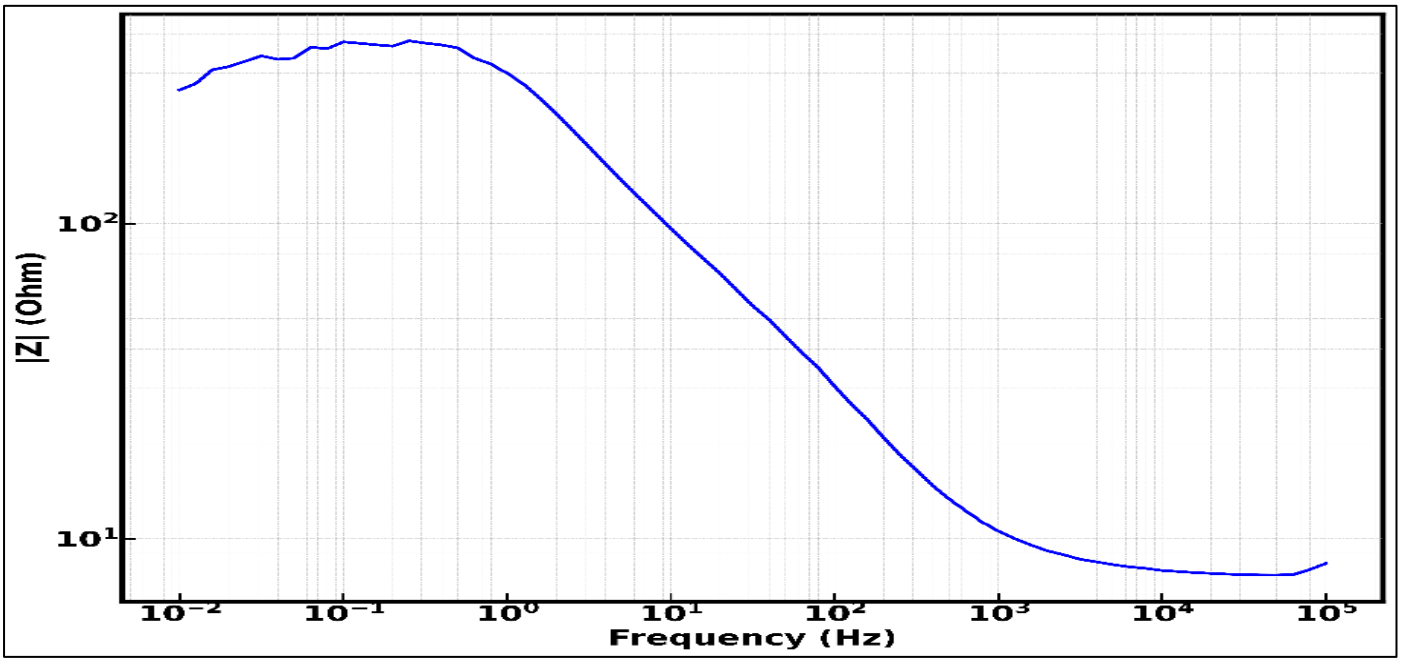

Fig 3 Bode Impedance Plot

- *Phase Angle Characteristics*

The Bode Phase Angle Plot shows some insight into how the passive film behaves capacitively and if it has defects within the passive film. In this case the phase angle for the film reached a high point of approximately 43–45 degrees at mid-range frequency (1–100 Hz) which indicates the presence of a non-ideal capacitive behavior that would be present with a defective passive layer. Compared to a fully protective passive layer (which typically will show phase angles near –80°), the lower phase angle exhibited by this passive film clearly illustrates that the passive film that was formed on the WAAM AA7075 Nano-TiC composite exhibits heterogeneity and porosity in its structure as indicated in Figure 4. These behaviors are due to nano-TiC particle interfaces and WAAM induced micro-porosity and localized compositional variations in the aluminum alloy matrix. At low frequencies, the negative phase angle values suggest the dominating reaction mechanisms of the film involve faradaic reactions; therefore, there is an increased potential for localized corrosion phenomena (pitting).

ISSN No:-2456-2165 https://doi.org/10.38124/ijisrt/26feb1444

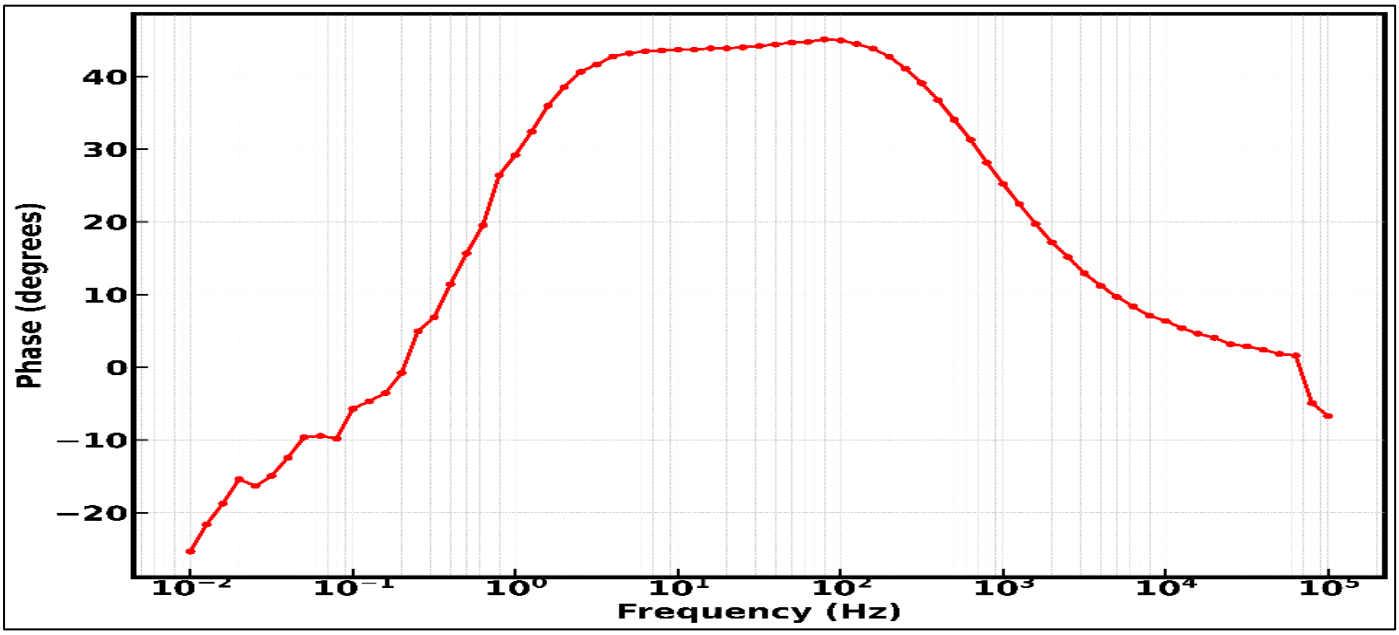

Fig 4 Bode Phase Angle Plot

- *Equivalent Circuit Model for AA7075 Nano-TiC MMC*

The EIS results depicted that the WAAM composite had smaller impedance modulus values as a result of decreased charge transfer resistance at low frequencies. The phase angles revealed that the passive film exhibited less stability than the passive film on the wrought AA7075 due to the inherent porosity and the heterogeneity of the WAAM processed composite. The EIS data were modeled using an equivalent electrical circuit with two time constants; the model consisted of the solution resistance (Rs), a constant phase element (Q1) in series with the passive film resistance (R1), and another series combination of charge transfer resistance (R2) and constant phase element (Q2) as indicated Figure 5. The two combinations of elements represented the non-ideal electrochemical behavior of the passive film formed on the WAAM fabricated AA7075-Nano-TiC composite. The measured EIS data show that the corrosion of the AA7075 Nano-TiC composite produced via WAAM can be described by an electrochemical model characterized by two time constants as indicated Table 2.

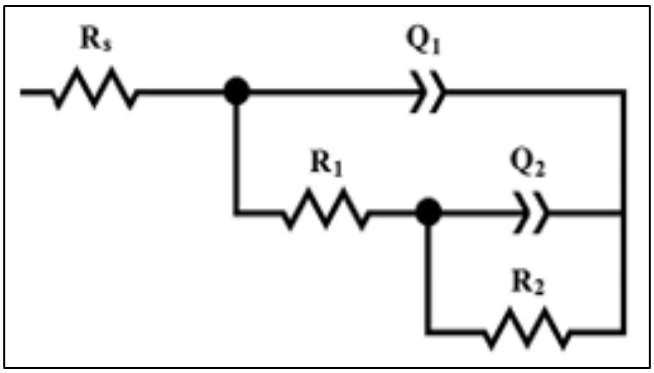

Fig 5 Equivalent Circuit Model for AA 7075 Nano-TiC MMC

Table 2 Equivalent Circuit Fitting Results of EIS Data.

Parameter	Value	Unit
R_s	11.8	$\Omega \cdot cm^2$
R1	1.45×10^2	$\Omega \cdot cm^2$
Q1 (Y_0)	2.9×10^{-5}	$\Omega^{-1} \cdot cm^{-2} \cdot s^n$
n1	0.86	–
R2	2.25×10^2	$\Omega \cdot cm^2$
Q2 (Y_0)	1.1×10^{-4}	$\Omega^{-1} \cdot cm^{-2} \cdot s^n$
n2	0.78	–

R_s represents the electrolyte resistance, and R1 as well as Q1 represent the real resistance and the non-ideal capacitive behavior of the passive oxide layer. The second time constant is represented by the resistances R2 and the capacitances Q2 and is related to the charge transfer in the electrolyte-metal interface through the porous regions and the reinforcement-matrix interfaces. A value of $n < 1$ shows that the behavior of the electrochemical double layer deviates from the ideal capacitive behavior due to the roughness of the surface and the heterogeneity of the structure due to the porosity and microstructural differences generated during the WAAM process.

- *Corrosion Mechanism from EIS*

The combined impedance and phase angle behaviors indicate that corrosion of the WAAM AA7075–Nano-TiC composite is influenced by both a defective passive film and charge transfer resistance. In addition to contributing to grain

ISSN No:-2456-2165 https://doi.org/10.38124/ijisrt/26feb1444

refinement via the presence of nano-TiC particles, these ceramic reinforcements can create local micro-galvanic couples between the reinforcement and the aluminum matrix when exposed to a chloride environment, thus locally reducing stability of the passive oxide layer.

➢ *SEM and EDS Analysis*

The SEM image and EDS data for the corroded WAAM-produced AA7075 – Nano-TiC composite exposed to a 3.5 wt% NaCl solution show evidence of pitting corrosion, compositional heterogeneity on the surface, the presence of oxygen-rich corrosion products, local Al depletion in the pit regions, and chemically inert TiC particles that may serve as the site of micro-galvanic action as indicated Figure 6.

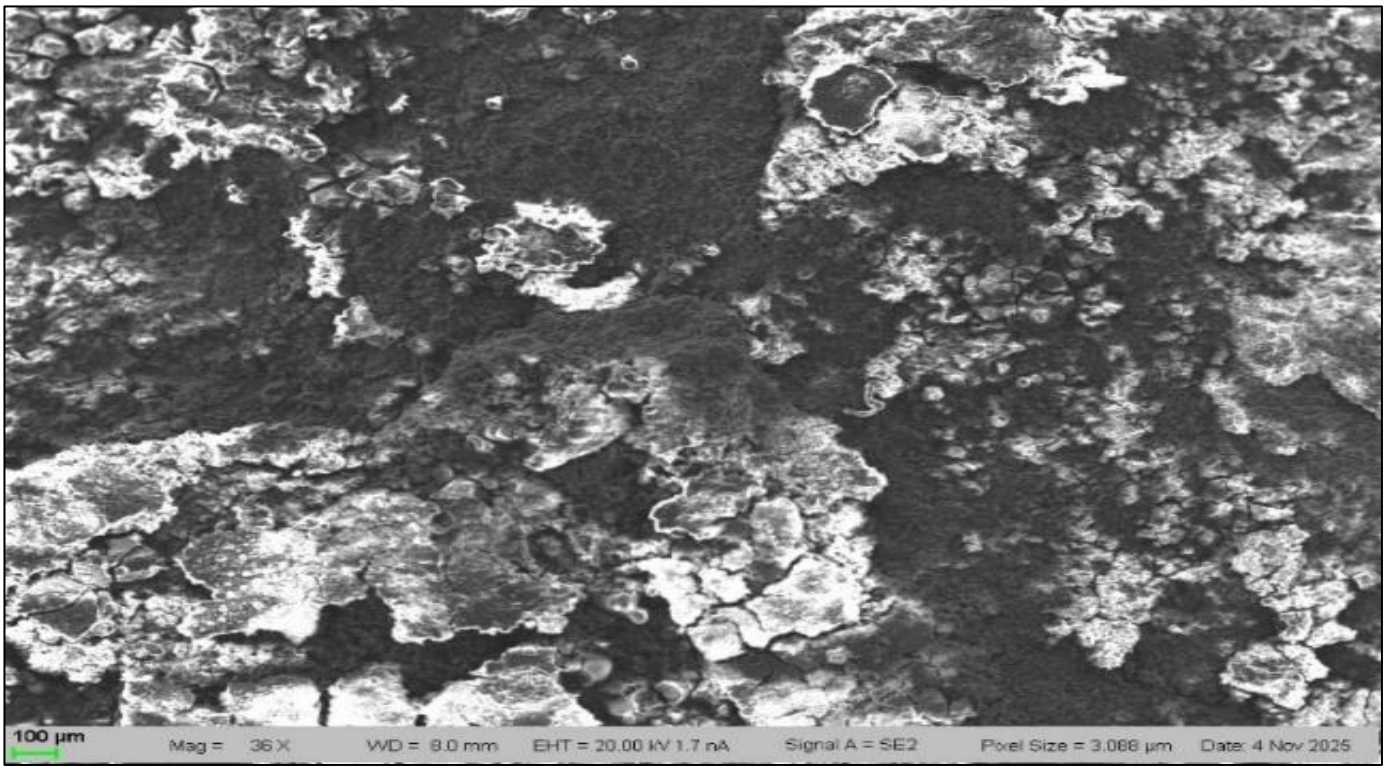

(a)

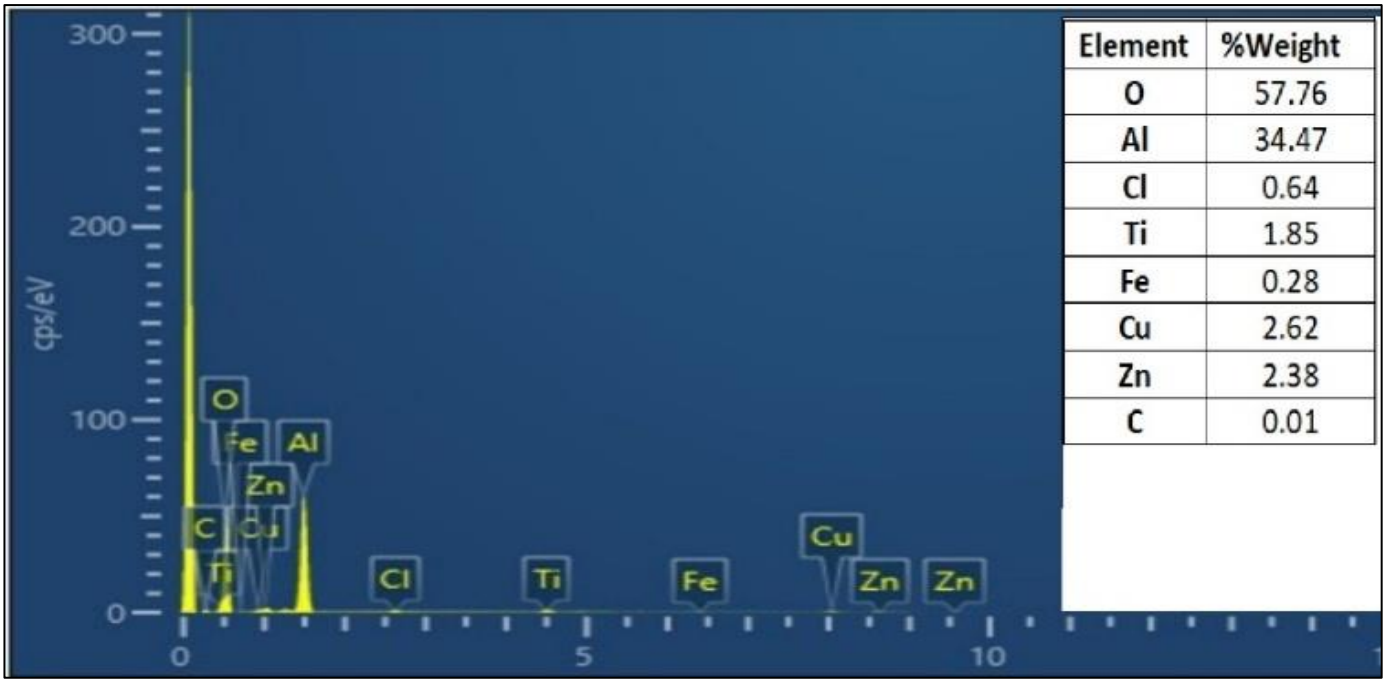

(b)

Fig 6 Corroded SEM-EDS Analysis AA7075 Nano-TiC Metal Matrix Composite

ISSN No:-2456-2165 https://doi.org/10.38124/ijisrt/26feb1444

D. Correlation Between EIS and PDP Results

The potentiodynamic polarization and electrochemical impedance spectroscopy results for the WAAM-processed AA7075-nano-TiC composite exposed to chlorides show good agreement in terms of their description of corrosion behavior. Bode plots were characterized as having a single depressed capacitive loop, and a single broad phase-angle maximum indicating a charge-transfer-controlled corrosion mechanism that is influenced by a non-ideal interfacial layer. The lower frequency impedance and charge transfer resistance indicate that the addition of nano-TiC has produced a partially protective surface film, consistent with the refined microstructure. However, the reduced phase angle and departure from ideal capacitive response indicate significant heterogeneity on the surface and at the interface, due to particle-matrix interfaces and microstructural heterogeneities inherent to the WAAM fabrication method. It appears that the microstructurally beneficial effects of nano-TiC reinforcement may not provide sufficient improvements in corrosion resistance, due to the localized nature of electrochemical reactions promoted by surface and interfacial heterogeneities. The polarization results further support this, showing that while passivation occurs, there is still not complete suppression of anodic dissolution in chlorides. Overall, these results suggest that the corrosion performance of WAAM-fabricated AA7075-nano-TiC composites is controlled by a balance between stabilization of the passive film and the degree of heterogeneity at the surface and interface; therefore, corrosion performance is improved moderately rather than significantly as indicated Figure 6 and 7.

The corrosion behavior is therefore governed by a trade-off between grain refinement benefits and reinforcement-induced galvanic activity, compounded by process-related porosity.

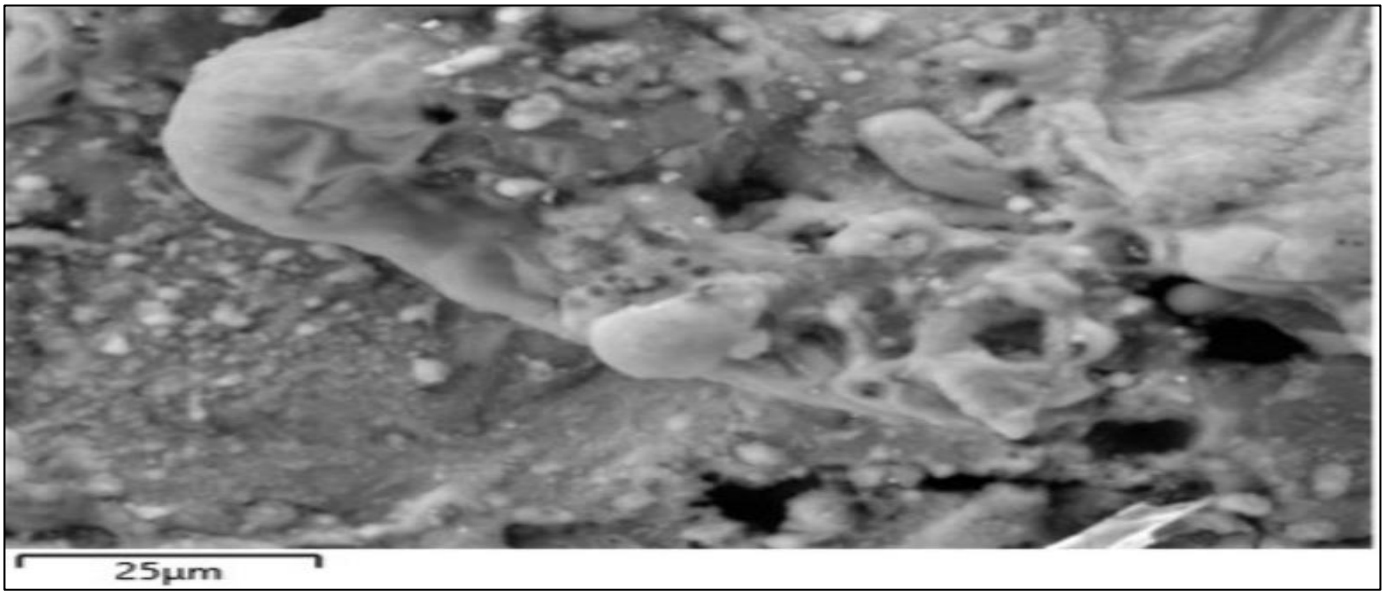

(a)

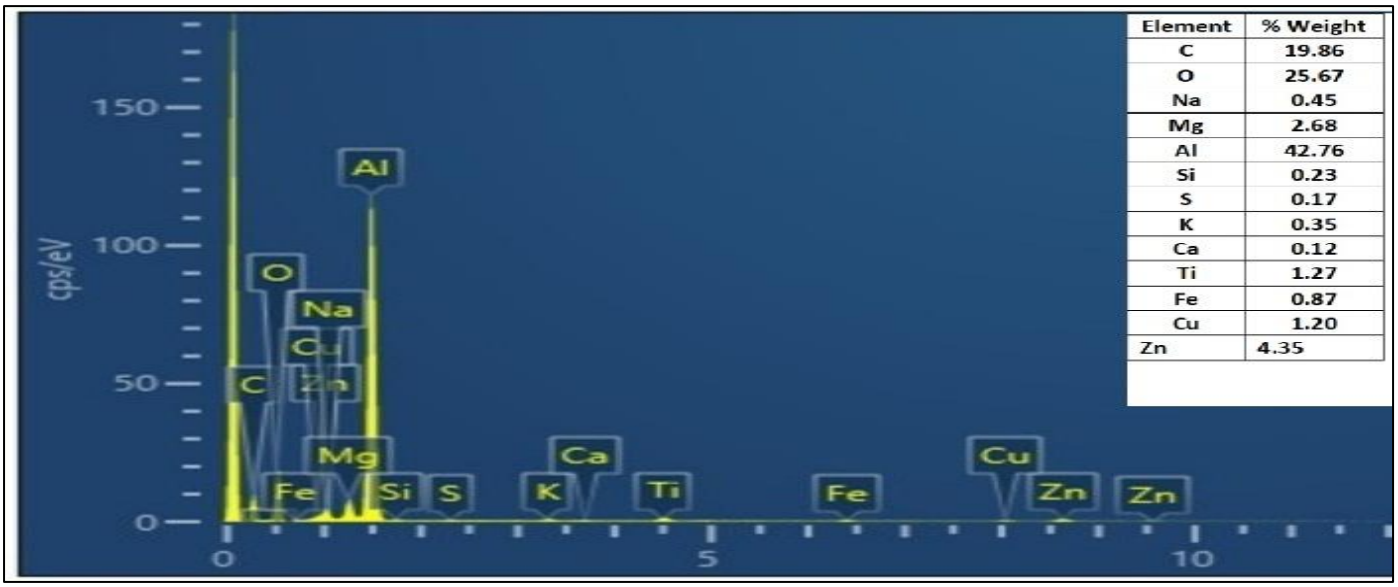

Element	% Weight
C	19.86
O	25.67
Na	0.45
Mg	2.68
Al	42.76
Si	0.23
S	0.17
K	0.35
Ca	0.12
Ti	1.27
Fe	0.87
Cu	1.20
Zn	4.35

(b)

Fig 7 SEM-EDS Analysis Uncorroded AA7075 Nano-TiC Metal Matrix Composite

ISSN No:-2456-2165 https://doi.org/10.38124/ijisrt/26feb1444

The overall corrosion behavior of the WAAM AA7075-Nano-TiC composite is controlled by a mix of grain size reduction, distribution of nanoparticles, and development of secondary phases; Nano-TiC provides the grain refinement but can provide preferred sites for localized corrosion to initiate where passive film continuity has been disrupted. Additionally, the non-equilibrium solidification and residual stress that are produced during the WAAM process, will increase localized corrosion in a chloride environment.

The SEM micrograph of the corroded WAAM-fabricated AA7075–nano-TiC composite exposed to 3.5 wt.% NaCl solution exhibited significant surface damage including both localized pitting and dissolution characteristics. The corroded surface was very irregular and demonstrated distinct pit morphologies; sharp-edged pits and undercut regions were characteristic of localized failure of the passive film coating on the surface rather than uniform corrosion of the surface. Additionally, the pits did not exhibit a regular distribution throughout the surface but appeared to be located primarily around surface asperities, small pores created during the WAAM process, and the interfaces of the reinforcement material and matrix. The corrosion pits were examined under high magnification and found to exhibit evidence of localized matrix dissolution with the resulting surface being porous and irregular with corrosion products accumulated within the cavity of each pit. The evidence of these features demonstrates that the primary locations of initial corrosion pit development occur based on the microstructural heterogeneities present in the AA7075–nano-TiC composite; specifically, areas of localized TiC particle agglomeration, intermetallic phases and the solidification boundaries formed during the WAAM fabrication process. It has been concluded that micro-galvanic effects occur when the aluminum matrix reacts with the ceramic reinforcement or secondary phases resulting in local instability of the passive film in a chloride containing environment. Correspondingly, the EDS analysis of the corroded regions showed increased oxygen content, which correlates with the formation of corrosion products including aluminum hydroxide and aluminum oxides. Conversely, the relative aluminum content within the corrosion pit area decreased due to active dissolution of the matrix. Localized trace enrichment of alloying elements Cu, Fe and Zn occurred as well, which was caused by their lower dissolution rate compared to aluminum, and their tendency to persist as residual phases during corrosion. Indirect evidence of chloride-related species present in the corrosion products were detected via the corrosion morphology and chemistry. Ti remained detectable in the corroded regions demonstrating the chemical stability of the nano-TiC reinforcement during electrochemical exposure. However, the presence of Ti-rich areas in or near corrosion pits indicate that TiC particles can serve as cathodic sites which promote localized anodic dissolution of the surrounding aluminum matrix. This type of behavior supports the theory that, although the addition of nano-TiC reinforcement benefits the refinement of grains and increases hardness of the metal matrix composites, it may also facilitate localized corrosion through galvanic reactions. The SEM – EDS data clearly demonstrate a strong correlation with the potentiodynamic polarization results. Specifically, the presence of localized pits and corrosion product-filled cavities provide direct microstructural evidence supporting the observed increase in anodic current density and susceptibility to pitting corrosion suggested by the polarizationcurves.

In addition, the surface morphology observed post-corrosion correlated well with the EIS data. The low impedance modulus at low frequencies and depressed phase angle maxima suggest the existence of a defective and non-uniform passive layer, which was confirmed by SEM through the presence of discontinuous oxide films and pit-dominant surface degradation. The two time constants identified in the equivalent circuit model represent the compromised passive film and the charge transfer processes occurring within the pits and porous corrosion product layers.

Therefore, the SEM – EDS examination of the corroded surface confirms that the corrosion behavior of the WAAM processed AA7075 – nano-TiC composite is controlled by localized passive film break down, micro-galvanic reactions and WAAM induced surface heterogeneity. These micro structural characteristics provide a direct mechanistic basis for the moderately resistant corrosion behavior and localized corrosion sensitivity of the WAAM processed AA7075 – nano-TiC composite to corrosive media as inferred from the results of the combined PDP and EIS studies.

IV. CONCLUSIONS

The corrosion behavior of wire arc additive manufacturing (WAAM) processed AA7075-Nano TiC metal matrix composite has been examined systematically and concluded.

- WAAM has led to a finer grain structure than unreinforced AA7075 material, with an increased proportion of high angle grain boundaries as a result of the rapid solidification of the weld pool and the reinforcement by nano TiC particles.
- A marginal improvement in corrosion potential compared to unreinforced AA7075 material, but an increase in the propensity to undergo localized corrosion due to the heterogeneous nature of the microstructure was observed using potentiodynamic polarization studies.
- Analysis using electrochemical impedance spectroscopy (EIS) showed a decrease in the charge transfer resistance and a less stable passive layer formed on the surface of the WAAM composite in a 3.5% w/w NaCl solution. In addition to their effect on grain size refinement, nano TiC particles are also able to enhance the micro galvanic effects occurring at the matrix-reinforcement interfaces.
- The corrosion properties of WAAM processed AA7075 – Nano TiC composites are primarily determined by porosity induced during the fabrication process, the spatial distribution of the reinforcements and the formation of secondary phases.

This study has provided essential information on the corrosion processes occurring within the fabricated materials, and the results obtained may provide useful information for

ISSN No:-2456-2165 https://doi.org/10.38124/ijisrt/26feb1444

the optimization of the WAAM fabrication process to produce materials with enhanced corrosion properties.

REFERENCES

[1]. Gibson I, Rosen D, Stucker B, *Additive Manufacturing Technologies*, Springer, 2015.
[2]. DebRoy T et al., Additive manufacturing of metallic components, *Prog Mater Sci*, 2018.
[3]. Frazier WE, Metal additive manufacturing: A review, *J Mater Eng Perform*, 2014.
[4]. Herzog D et al., Additive manufacturing of metals, *Acta Mater*, 2016.
[5]. Williams SW et al., Wire + arc additive manufacturing, *Mater Sci Technol*, 2016.
[6]. Martina F et al., WAAM of structural alloys, *J Mater Process Technol*, 2019.
[7]. Ding D et al., Wire-feed additive manufacturing of metals, *Int J Adv Manuf Technol*, 2015.
[8]. Ding J et al., Large-scale WAAM components, *Robot Comput Integr Manuf*, 2016.
[9]. Wu B et al., Corrosion behavior of WAAM Ti–6Al–4V, *Corros Sci*, 2018.
[10]. Zhang L et al., Corrosion of WAAM Inconel alloys, *J Alloys Compd*, 2020.
[11]. Gu J et al., WAAM of aluminum alloys, *Mater Des*, 2017.
[12]. Davis JR, *Aluminum and Aluminum Alloys*, ASM International, 1993.
[13]. Birbilis N, Buchheit RG, Electrochemical characteristics of AA7075, *J Electrochem Soc*, 2005.
[14]. Ralston KD, Birbilis N, Effect of grain size on corrosion, *Scr Mater*, 2010.
[15]. Suryawanshi J et al., Additive manufacturing of aluminum alloys, *Mater Sci Eng A*, 2017.
[16]. Guo C et al., Corrosion behavior of additively manufactured Al alloys, *Mater Res Express*, 2021.
[17]. Miracle DB, Metal matrix composites, *Compos Sci Technol*, 2005.
[18]. Prasad SV, Asthana R, Aluminum metal matrix composites, *Tribol Lett*, 2004.
[19]. Zhang Z et al., Nano-TiC reinforced aluminum composites, *Mater Sci Eng A*, 2018.
[20]. Liu Y et al., Corrosion of particle-reinforced MMCs, *Corros Sci*, 2019.
[21]. Tang Y et al., Corrosion behavior of AM alloys, *J Mater Eng Perform*, 2021.
[22]. Juillet C et al., Effect of porosity on corrosion, *Corros Sci*, 2018.
[23]. Frankel GS, Pitting corrosion of metals, *J Electrochem Soc*, 1998.
[24]. Abioye TE et al., Corrosion of WAAM clads, *J Mater Process Technol*, 2015.
[25]. Silva CC et al., Passive film stability in AM alloys, *J Alloys Compd*, 2016.
[26]. Ghaffari M et al., Mechanical behavior of WAAM alloys, *Addit Manuf*, 2021.
[27]. Vacchi S et al., Microstructure evolution in WAAM, *Metals*, 2021.
[28]. Tejonadha Babu K et al., Corrosion of MMCs, *Mater Sci Forum*, 2019.